1

An Overview of Star Formation

1.1 Introduction

Within our current understanding of star formation as observed through the lens of molecular astronomy, we can identify the following as the most significant areas of contemporary research: prestellar cores, hot cores and hot corinos, accretion and protoplanetary disks, photodissociation regions, stellar jets, disk winds, outflows, and masers. Of course, these sit within the wider considerations of dense molecular clouds on many scales, from the giant molecular clouds (GMCs) to fragments, filaments, and clumps. In turn, our understanding of molecular clouds depends on our understanding of molecular excitation, energy balance, gas and grain surface reaction kinetics, cosmic ray ionisation, and photochemistries. Some of these facets are more appropriate to low-mass star formation regions (LMSFRs), some to their high-mass equivalents (HMSFRs). While theoretical understanding of low-mass star formation (up to 2 $M_{\odot}$.) is currently quite well constrained, that of high-mass stars (>10 $M_{\odot}$) is only now emerging with the help of the latest high-resolution telescopes that offer acutely focused observations as well as deep field surveys of multiple sources at great distances.

All the steps along the way to star formation sit in an evolutionary schema that starts in molecular clouds concentrated particularly in the spiral arms of the disks of galaxies such as our own. However, rates of star formation even in the Milky Way differ in different regions. For example, rates are slower in the Taurus clouds, much more rapid in Orion or W3 or W49. Observations show even more vigorous star formation rates in some external galaxies, such as the 30 Doradus region in our close neighbour the Large Magellanic Cloud (LMC), and in more distant 'starburst galaxies' such as NGC 253 or Arp 220.

With few exceptions stars form in clusters, in anything from ten to a million or more in relatively close proximity. A cluster of high-mass stars (an OB

https://doi.org/10.1017/9781009277433.002 Published online by Cambridge University Press

association) may occupy a volume of space defined by just a few tens of parsecs early on in its main sequence life, but it will progressively spread to cover a region likely to be hundreds of parsecs wide. OB stars burn out in a few tens of million years, having driven apart their clustered near neighbours through radiation pressure, mechanical turbulence, gas dispersion, and rapid reductions in gravitational stability. They also scatter many lower-mass stars whose formation they will have triggered, although these smaller stars linger to evolve much more slowly. We see such distributions in Orion, Upper Scorpius , and Upper Centaurus-Lupus. These local clusters that are still embedded in their parent molecular cloud cores are obviously at an early stage of evolution, shrouded in dust and often observable only at infrared wavelengths. We will look at surveys of such clusters, as well as the examples of Sgr B2, W43, and Orion BN/KL in the High-Mass Star Formation (HMSF) section. Cluster subgroups such as Orion 1a, 1b, and 1c are clear evidence of the recursive nature of sequential, self-propagating star formation in which the impacts of high-mass stars, expanding HII regions, stellar winds, and occasional supernova explosions lead to widespread gas compression and the triggering of fresh star formation. The Trapezium stars are another familiar example in the visible, along with the Pleiades, which mark the current end of a subgroup sequence of formation and destruction.

At its simplest, the evolutionary sequence for low-mass, solar-type stars proceeds from the diffuse interstellar medium (ISM) to dense cloud to collapsing prestellar core to protostellar envelope and accretion disk, before nuclear ignition and a main sequence lifetime ending in a planetary nebula re-seeding the ISM. In contrast, recent statistical analysis of multiple high-mass star formation regions shows quite clearly how the absence of low- and intermediate-mass stars associated with hot massive proto-cluster cores strongly suggests that high-mass star formation kick-starts the formation of lower mass stars which emerge subsequently. It seems likely that high-mass clusters are triggering the collapse of cold dense prestellar cores, which themselves fragment and engender the binary and multiple stars we observe in two-thirds of solar mass main sequence systems. Let us add a little more detail to that overview, starting for simplicity, if not stellar formation logic, with the low-mass case.

Low-Mass Star Formation (LMSF)

1.2 Diffuse Clouds

The average particle density in the interstellar medium (ISM) is about 1 cm^{-3}. Where the diffuse ISM is in temperature and pressure equilibrium with its surroundings, this neutral hydrogen (HI) gas forms diffuse clouds under gravity

https://doi.org/10.1017/9781009277433.002 Published online by Cambridge University Press

in which gas particle densities are low (a few tens per cubic centimetre) and temperatures moderate (80–100 K). We can also extend the diffuse cloud classification from the purely atomic to the diffuse, and the translucent, depending on overall column densities, molecular hydrogen to atomic hydrogen ratios, or even some CO (carbon monoxide) abundance. Size and scale vary considerably, but typically these clouds are ~0.5 pc in diameter and ~3 $M_{\odot}$ in total. They are optically thin to the interstellar radiation field, with column densities correlating with visual extinction A_v ~0.05 magnitude, and it is the penetration of Far Ultraviolet (FUV) radiation that determines their chemistry. The tenuous molecular composition of diffuse clouds is studied at submillimetre wavelengths through absorption (typically ground state lines) against strong background sources, often extragalactic. Even the highest column density clouds show principally diatomic molecules, and just a few triatomics, both neutral and ionised, dominated by the elements of hydrogen, carbon, and oxygen. The precise abundance of the overwhelmingly most common molecule, H_2, is determined by the balance between its accretion, diffusion, and reaction rates on the surfaces of dust grains in competition with the rate of impinging photo-dissociating UV. Given the effectiveness of photodesorption processes, dust surfaces in diffuse clouds are regarded as essentially clean of molecular species for most of the cloud's diffuse lifetime.

1.3 Molecular Clouds

About 80 per cent of the molecular hydrogen in our Galaxy exists, however, in the much denser conditions of GMCs, each with masses commonly over 10^6 $M_{\odot}$. These enormous self-gravitating reservoirs of molecular gas and dust are where stars in the Milky Way exclusively form, although at a gas conversion efficiency rate of only ~5 per cent due to the multiple complex internal shock, turbulence, and radiation dynamics arising from star formation (particularly HMSF) that disrupt the localised continuity of gravitational collapse and gas coalescence. In classifying what we will find in our case studies to be far from homogenous molecular cloud conditions, we can generalise to the extent of noting that GMC column densities do average over 10^{22} H-nuclei cm^{-2} and show visual extinctions up to A_v ~8 magnitude. Remember, these are broad averages, and we will be identifying much higher-density locations within GMCs in some of the case studies that follow.

As in the diffuse cloud case, the thermal balance within a GMC determines its stability, and we will look at this in a little more detail in Chapter 6. Photoelectric effects dominate in the outer regions, while cosmic ray heating and local turbulence are most significant in the inner regions . However, dense

https://doi.org/10.1017/9781009277433.002 Published online by Cambridge University Press

molecular clouds are typically cold (~10 K). This is because the gas is predominantly molecular and, with the exception of H_2 (which has no dipole moment), molecules typically have many available rotational levels through which collisional energies are radiated. The kinetic energy of molecular gas is therefore efficiently reduced in comparison with an atom-dominated cloud. Balancing abundance against cooling efficiency, ^{12}CO offers the greatest cooling contribution in lower-density molecular conditions ($<10^3$ cm^{-3}). At higher densities, the ^{12}CO transitions become optically thick and the cooling efficiency of the less common isotopologue, ^{13}CO, can compete, as can that of certain molecular ions and neutral hydrides, including H_2O.

Where FUV photons penetrate molecular clouds, they ionise, dissociate, and heat the gas. Atomic H ionising photons are absorbed in a thin transition zone (column density ~10^{19} cm^{-2}) in which almost fully ionised atomic gas becomes almost fully neutral. FUV photons with energies <13.6 eV dissociate H_2 but ionise C, so an HI/CII region forms the next 'layer'. In dense photodissociation regions (PDRs), dust at visual extinction A_v ~4 magnitudes marks the H_2 front, and beyond that come C/CO zones. This is a simplification of reality, as the case studies in Chapters 14 and 15 will show. However, where dust grains within GMCs are protected from externally impinging FUV, here the gas and dust temperatures drop, and gas-phase chemistry is now driven, as we noted, by cosmic ray ionisation that initiates complex ion–molecule reaction networks. Within such a dark cloud, the dust-grain surfaces become the sites of migration and reaction between atoms and radicals, with gas–grain exchange through accretion and desorption. With progressive cooling during cloud collapse, ice layers accumulate as storehouses of the gas–grain molecular products, many of which are saturated and/or complex, only to be released if and when the gas and dust are subsequently warmed by star formation activity.

1.4 Dense Prestellar Cores

Against the gravitational forces within a cooling dense molecular cloud, turbulent motions from a variety of processes both disrupt and amplify existing inhomogeneities in gas and dust distribution, resulting in the formation of extra-dense filaments. The densest of these (on a scale ~0.1 pc) may collapse under their own gravity, forming a central nascent protostar with an accretion disk (radius ~ ten thousand AU). The disk actually expands over time, with magnetic braking working against the conservation of angular momentum while continuing accretion onto the central protostar is enabled through

https://doi.org/10.1017/9781009277433.002 Published online by Cambridge University Press

an energy balance maintained by jets and outflows (disk winds) emerging from the central object perpendicular to the disk plane.

Prior to any appearance of a nascent protostar within a central density peak, the initial dense , cold core has a typical gas-phase particle density of 10^6–10^7 cm^{-3} and temperature ~10 K. In Chapter 3 we will meet the many cores of the Ophiuchus molecular cloud with characteristic sizes of several thousand AU. At this point, on a scale at which the current generation of interferometers has really come into its own, we might ask what is it that is so valuable that is gleaned from the higher resolution of the molecular composition of accretion disks and their associated winds? After all, could any of these molecular species survive the disruption, dispersal, and material aggregations that follow stellar ignition? We must look to the outer reaches of protoplanetary disks and later in their evolutionary development for circumstances favourable to molecular formation chemistries that might produce the molecular species we currently observe in the fleeting passage of outer Solar system objects close to Earth. However, in the early stages of star formation, in trying to understand the multiple steps associated with that formation process, molecular emission tells us much about the physical conditions of each stage, all of which will become clearer through the case study examples to follow.

Along with the many smaller molecular species observed in the gas phase of cold, dense prestellar cores, there are complex carbon molecules offering direct evidence for active microscopic dust grain surface chemistries. Also evident is deuterium fractionation , and these observations collectively give distinctive clues as to core conditions of temperature, density, and radiation flux. Ices are also widely observed in absorption towards many reddened background stars, having accumulated on the surface of dust grains. H_2O ices are known to begin accumulating at densities ~10^3 cm^{-3} and temperatures ~15 K. Other ices, such as CH_4, NH_3, and some CO_2, also start to freeze out under these conditions with rapid increases as the core collapses and particle densities increase. Alternative routes for these simple saturated molecules to form in the gas in the quantities observed are woefully inefficient. Rather, the molecules are undoubtedly forming on grain surfaces through elemental reactions, including ubiquitous successive hydrogenation.

By the time the collapsing core reaches a gas-phase density ~10^5 cm^{-3}, the dominant volatile carbon species, CO, is undergoing rapid depletion onto the grains. This abrupt large-scale freeze-out of CO produces a distinct H_2O-poor (apolar) ice phase which has been observed directly as well as re-created in laboratory analogues. This CO-rich ice reacts with, among other species, atomic H to form H_2CO and CH_3OH – molecules we shall meet repeatedly in the case studies to follow, along with even more carbon-based complex organic

https://doi.org/10.1017/9781009277433.002 Published online by Cambridge University Press

molecules (COMs). We can reiterate that these species are certainly not made efficiently through collisional gas-phase reactions alone. However, this is cold carbon-chain chemistry, not to be confused with a warm carbon-chain chemistry (WCCC) that we will also find associated with low-mass protostars at a later stage of their evolution. For theorists and modellers, a major puzzle of recent years has been by what process or processes the COMs observed in the gas phase are actually desorbed from grain ices. The dust temperatures are deemed too low for thermal desorption, yet non-thermal processes such as photodesorption, cosmic-ray-induced spot heating, or localised exothermic reaction desorption give unsatisfactory results in any but species-specific cases. This is where current laboratory research into ice analogues will prove of crucial interest.

To pick up on the deuterium fractionation evidence, it is characteristic of cold prestellar cores that they have a high abundance of deuterated molecules such as DCO^+, DCN, and HDCO, with ratios to their undeuterated counterparts at least three orders of magnitude higher than the overall [D]/[H] ratio (which is $\sim 2 \times 10^{-5}$ in the ISM). Even doubly and triply deuterated species have been observed. The reasons for their abundance are that their formation reactions are exothermic and therefore efficient in such cold conditions, while the dominant destruction pathway for H_3^+ and H_2D^+, the principal initiators of fractionation, involves CO which by this stage, as we said, is quickly freezing out. Chapter 3 will reconsider deuteration in more detail. Chemical modelling suggests a lifetime for the cold, dense prestellar freeze-out phase of about 10^5 years before we next identify distinctive protostellar characteristics. For those unfamiliar with the many molecular species introduced throughout the following chapters, Appendix A directs the reader to some conveniently tabulated data.

1.5 Cold Protostellar Envelopes

Prestellar cores emit at infrared and longer wavelengths. Collapse of the core progresses, with the gravitational free-fall time extended perhaps by ambipolar diffusion and turbulence from within, irrespective of possible external influences such as shocks from neighbouring stellar activity. Once a central hydrostatic object coalesces within the core, we can say we have a protostar, and it will grow with accretion of surrounding envelope material from the engendered circumstellar disk. We will see in the LMSF chapters that protostellar envelopes are detected through millimetre-wave dust continuum emission, luminosities being roughly proportional to the total mass of dust in the

https://doi.org/10.1017/9781009277433.002 Published online by Cambridge University Press

envelope. Centimetre-wave radio continuum detections arise from accretion shocks at the protostellar surface, this luminosity being proportional to the total luminosity of the star, and envelope and protostellar masses can then be deduced from these luminosities. High ratios of millimetre-wave luminosity to total luminosity also show just how much the envelope mass may exceed that of the central protostar, through an accretion phase we expect to last up to 10^5 years. Infall motions themselves can be traced through molecular and molecular ion rotational lines, and both red and blue shifts are observed along the line of sight resulting from the large-scale rotation of the envelope gas around the protostar.

Within an opaque protostellar envelope, very close to a low-mass protostar, small (<100 AU), warm, dense regions have been discovered in recent years, designated 'hot corinos', the prototypical example being that associated with IRAS 16293-2422 which we will examine in Chapter 3. This gas is rich in complex organic molecules (COMs) – those with at least six atoms – with line profiles suggesting the emission arises from the inner surface of the accretion disk. However, while the disks themselves can have lifetimes of several million years, hot corino observations seem limited to the earliest stages of accretion disk evolution, and it seems likely that the complex organics are quite quickly degraded to CO in the warm gas as the protostar evolves.

1.6 Jets and Disk Winds

Along with the accretion disk itself, protostellar systems typically show outflow activity in which some of the accretion energy converts to kinetic energy in a collimated bipolar jet or disk wind. The nearby Perseus molecular cloud, for example, which we will meet in Chapter 4, shows hundreds of jets associated with embedded protostars, which we can trace in rotationally excited H_2 as well as emission lines from SiO, SO, and CO. These outflows generate turbulence in the surrounding envelope, driving their dispersal, and effectively limiting the available accretion mass. Equally, outflows can drive shocks that may well trigger star formation in neighbouring clouds and, especially in the high-mass case, account for the tendency for stars to form in clusters. Wherever the velocity of ejected material exceeds the sound speed, the surrounding gas and dust cannot respond dynamically until the material arrives. When that happens, the shocked gas is compressed, heated, and accelerated before subsequently cooling through line emission, and these changes in conditions are reflected in observable changes directly to the gas phase and to

https://doi.org/10.1017/9781009277433.002 Published online by Cambridge University Press

its composition resulting from the sputtering of ices. While H_2 and CO, as so often, are the dominant coolants, the common shock indicators in molecular clouds close to emerging stars are H_2O, SiO, SO, and SO_2, which we will meet particularly in the HMSF sources.

1.7 Protoplanetary Disks

As we will see when we look at specific examples, the impinging FUV (Far Ultraviolet), EUV (Extreme Ultraviolet), and X-ray stellar radiation emerging from the protostar creates dense photodissociation conditions at a disk's inner surface. Deeper into the disk, the magnetised gas is turbulent and grain collisions promote growth into larger aggregates, which is how planet formation begins. Accretion continues, jet and disk outflows drive strong shock waves into the disk and envelope, small shock-heated knots called Herbig–Haro (HH) objects appear where jets impact surroundings, and broad, diffuse lobes of high-velocity ambient gas are swept up and accelerated to high velocities. With the dispersal of the envelope cloud, the protostar and disk become visible, and we have what are called T Tauri stars ($<2\ M_\odot$) or Herbig AeBe stars if larger ($2–8\ M_\odot$). Total accretion timescales are ~2 Myr, while disk dissipation takes ~3 Myr. With a variety of evolutionary stages, the timescale for low- and intermediate-mass stars to reach the main sequence is of order 10–100 Myr respectively.

Observations of the transition from accretion disk to protoplanetary disk have begun to be made possible by the latest high-resolution instrumentation. Close to a star, densities and temperatures are high and chemical equilibrium conditions rapidly attained. Further out from the star, differing conditions engender zones of particular molecular mixes before freeze-out onto cold grains at the outer margins. While gas–grain interactions dominate in the icy mid-plane, there is turbulent diffusion mixing material vertically and radial transport moving material laterally in the longer term. Dust grains will collide, stick, and potentially grow into aggregates. In several case studies we will look at key micro-chemical gas–grain processes occurring in the various molecular zones that undoubtedly do precede any aggregation of dust that might initiate planetesimal formation. Any subsequent evolution towards larger aggregations having a gravitational impact sufficient to engender, say, kilometre-size planetesimals that precede the formation of those planets that we now see associated with at least five thousand stars in our own Galaxy is a question for study elsewhere. The schematic of Figure 1.1 summarises the stages of low-mass star formation, giving spatial and temporal estimates.

https://doi.org/10.1017/9781009277433.002 Published online by Cambridge University Press

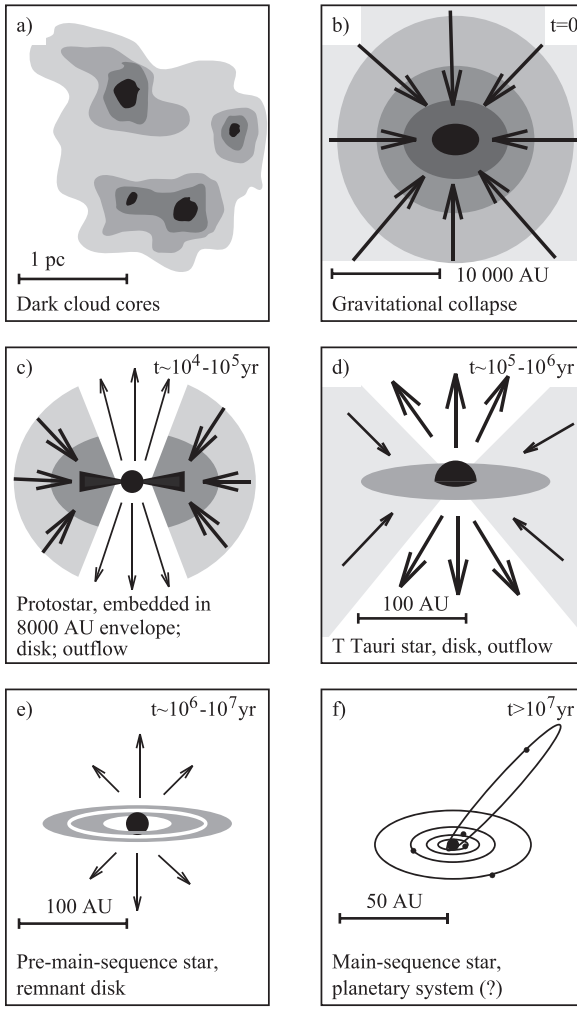

Figure 1.1 Schematic of the low-mass star formation process, with order-of-magnitude spatial and temporal scales (Hogerheijde 1998, based on Shu et al., 1987).

High-Mass Star Formation

1.8 Dark Cloud to Main Sequence

To reiterate, low-mass stars are of solar mass or less and not more than 2 $M_\odot$; intermediates are classified as between 2 $M_\odot$ and 8 $M_\odot$; and high-mass stars anything between 10 $M_\odot$ and 150 $M_\odot$ (at the theoretical extreme). Although

https://doi.org/10.1017/9781009277433.002 Published online by Cambridge University Press

the combined luminosities of high-mass stars in any galaxy dominate the total luminosity, their lifetimes are short in astronomical terms. Given the Galactic initial mass function (IMF), there are intrinsically fewer of them and, from the observer's perspective, they are generally further away (typically of order several kiloparsecs) than the average sample of low-mass stars. However, the development of ever higher-resolution instrumentation has increasingly allowed investigation of HMSFRs within, and even outside, our own Galaxy in ever greater detail. The James Webb Space Telescope launched in the last week of 2021 is just the latest in that line of development spanning the past fifty years.

With the observational constraints to date, there is as yet no entirely agreed-upon scenario for the formation of high-mass stars with quite the assurance we have just described for low-mass stars. The observations we do have and the theory both suggest that high-mass star formation takes place over a few 10^5 yr. High-mass protostars once formed also reach the main sequence over a comparable timescale while still embedded within their parent molecular cloud. Since they also invariably form in clusters, study of an individual high-mass star in relative isolation is an additional difficulty, so the overall challenge of HMSF studies is appreciable.

The physical complexity of an evolving HMSFR cluster is matched by the chemical complexity observed at millimetre and submillimetre wavelengths, so for the observer we can choose to adopt a four-stage categorisation of detectable evolutionary development. First, a gravitationally collapsing molecular cloud will fragment, with protostars forming in the cold, dense clumps. With typical temperatures ~10–20 K, these are only seen in extinction in the near- and mid-IR but seen in emission at far-IR and submillimetre wavelengths. Many of them are classified as Infrared Dark Clouds (IRDCs), sitting in front of diffuse background emission from the Galactic disk. Secondly, with collapse continuing, accretion disks and bipolar outflow systems form, and protostar heating raises the temperature of the envelope cloud. Continuing accretion boosts both protostellar mass and luminosity, bringing the protostar into visibility at infrared wavelengths. At this point, we have what is called a high-mass protostellar object (HMPO), characterised by high bolometric luminosity (>100 $L_\odot$), strong thermal dust continuum, but only weak centimetre emission.

Thirdly, as the envelope temperature increases and molecular ice species on the dust grain surfaces evaporate, they initiate a rich chemical gas-phase mix in a so-called hot molecular core (HMC). While HMPO environments may show some similarities with conditions associated with HMCs, the chemical composition of the gas around HMCs is richer due to higher temperatures.

https://doi.org/10.1017/9781009277433.002 Published online by Cambridge University Press

Why? Because, by definition, HMPOs are protostellar: they never reach a nuclear fusion stage. While not only warming their surroundings less than is evident in a YSO case, HMPOs never evolve sufficiently to emit ionising radiation. In contrast, as a massive object which has reached the YSO stage continues to accumulate matter, a fourth developmental stage after the HMC is observable, following from the increasingly strong radiation that dissociates and ionises the surrounding envelope gas. This is the evidence of ionised atomic hydrogen (HII), seen first in hypercompact (HCHII) regions which increase in size to ultra-compact (UCHII) region scale, emitting strong free–free emission at centimetre wavelengths. With the massive YSO remaining embedded within its natal cloud, the four stages are snapshots of a continuous evolution. Also, given that high-mass star formation typically occurs in clusters, it is not surprising that HMCs are commonly observed adjacent to UCHII regions, where one star in the cluster is likely to be more evolved than its immediate neighbour, detailed examples of which will be described in Chapters 11 and 12.

Among possible HMSF scenarios, it may be that the reality is closely similar to that of its low-mass stellar counterpart, with high-mass equivalents of dense cloud cores simply on a larger scale . In such a monolithic collapse scenario, the transition would be from dense molecular cloud core to protostellar envelope . However, since high-mass stars reach the main sequence in just a few hundred thousand years, one consequence of an accumulation of extremely large quantities of matter through rapidly accelerating accretion could be that the resulting high luminosity stops or even reverses the process through radiation pressure. That assumes a practically all-encompassing envelope, but if accretion were exclusively via an equatorial planar disk the majority of luminosity would not be trapped, and so the scale of resulting star not limited. This kind of competitive accretion seems the most likely scenario. One earlier suggestion, that of the collisional coalescence of stars already forming within a dense cloud, now seems very unlikely given a lack of sufficient stellar density within observed clusters.

1.9 Hot Cores

Closely associated with luminous high-mass stars are HMCs, compact (<0.1 pc) regions of warm (>100 K), dense (>10^7 cm^{-3}) gas. However, most are not yet well resolved, and there are others clearly energised in other ways. The archetypal Hot Core and its Compact Ridge companion in Orion, first studied in detail 30 years ago, is a case in point, being associated rather

https://doi.org/10.1017/9781009277433.002 Published online by Cambridge University Press

with the explosive decay of a multiple-star system, presenting features that are externally heated clumps, as we shall see in Chapter 9. The hot core in G34.26, described in Chapter 12, is equally intriguing for different reasons. Among the general discoveries of hot core chemistry, we can observe that nitrogen-bearing molecular species (such as HCN and CH_3CN), oxygen-bearing species (such as H_2CO), and sulphur-bearing species (such as SO and SO_2) are ubiquitous. HMCs offer the richest and most complex chemistries observed at millimetre wavelengths, with distinctions between oxygen-bearing and nitrogen-bearing species observed in a variety of hot core structures.

For the molecular astronomer, what makes hot cores particularly fascinating is the presence of high abundances of saturated (fully hydrogenated) species in the gas phase, including many COMs that are undoubtedly formed through grain-surface reaction networks as well as gas–grain interchange. The prototypical hot core G29.96-0.02 is also one that shows clear evidence of bulk rotation and nearby bipolar outflows from its associated star which have a likely influence, examined in Chapter 8. One of the COMs species that we will look at in detail in Chapter 12, and meet repeatedly elsewhere, is methyl cyanide (CH_3CN), which is a particularly useful tracer in delineating kinematical structure as well as higher temperatures in HMC objects. The chemistry of COMs, their origin and fate in warmed but cooling gas–grain circumstances, puts valuable constraints on modelling and observational interpretations. The high-resolution instruments now available, and those coming on stream in the near future, will undoubtedly reveal that the spatial structures within hot cores are likely to be a complex mix of components contributing to emission.

1.10 Compact HII Regions

High-mass stars may or may not begin hydrogen burning before accretion is complete, but surface temperatures, determined by accretion magnitudes and rates, can be sufficient to initiate ionising radiation. The flux of hydrogen-ionising photons may therefore generate an ionised hydrogen (HII) region while infall is still occurring. It seems likely that infalling material could compress the emergent HII region close to the stellar surface, forming a hypercompact (HCHII) region, until the balance between infall decrease and ionising photon flux increase leads to expansion of the ionised gas volume and formation of an ultracompact (UCHII) region. In simple circumstances the expansion is only halted when pressure equilibrium is reached between the ionised

https://doi.org/10.1017/9781009277433.002 Published online by Cambridge University Press

gas and the surrounding ISM; however, the reality of high-mass star formation clusters is that the mechanical energy of stellar winds outweighs that of thermal pressure, so HII regions are rarely neatly spherical structures. While the stellar UV is ionising hydrogen, the separated protons and electrons are subsequently free to recombine as neutral atomic hydrogen. Since only about one in three recombinations goes directly into the ground state, there is a subsequent cascade of radiative de-excitation detectable as line emission across a wide frequency range. These radio recombination lines (RRLs) are particularly useful to observers because they are largely unaffected by dust obscuration and provide kinematical, temperature, and density information for the ionised gas.

Given the complexity of forces behind the variety of compact HII structures, from the first IRAS space telescope observations in the infrared nearly four decades ago, it was clear that HII regions are not a homogeneous class of objects. Differing originating processes were characterised for the more evolved cases. Many have a 'cometary' appearance, meaning a dense leading edge and a more diffuse tail, as if generated by a star moving supersonically through its molecular cloud. G34.26+0.15 in Chapter 12 shows an archetypal cometary morphology. Alternatively, we might envisage the UCHII expansion into a region of rapidly reduced density, for example at the edge of a dense cloud, with an explosive 'champagne' escape flow resulting. A third possibility is that a massive star perhaps interacts with a clumpy molecular cloud and the ionised stellar wind becomes mass loaded by ablation and photoionisation of the clumps it passes through, terminating at a recombination (neutralising) front. Each schema has its theoretical justifications, and most HII regions are sustainable objects with masses ~1 $M_{\odot}$ over timescales ~10^5 yr. These regions typically have densities ~10^4 cm^{-3} on scales ~0.05 pc and, since they are deeply embedded in their parent envelope, no stellar luminosity directly escapes. We can observe them through its conversion into infrared radiation following heating and re-radiation from dust.

1.11 Photodissociation Regions (PDRs)

A variety of circumstances may result in the emergence of a photodissociation layer (sometimes also referred to as a photon-dominated region), but the most obvious is at the edge of a dense envelope that is subjected to an impinging stellar flux. This could be a reflection nebula subject to a relatively low radiation field (as Chapter 15 will show for the Horsehead Nebula in Orion), or it could be the edge of an HII region subject to a more powerful stellar field (as is the case for the Orion Bar in Chapter 14). While many of the physical

https://doi.org/10.1017/9781009277433.002 Published online by Cambridge University Press

and chemical processes within a PDR are closely similar to those in the atom-dominated ISM of diffuse and translucent clouds equally subject to photo-dissociating radiation, the PDR designation is usually applied specifically to the dense molecular cloud regions closest to bright, hot, high-mass stars. The PDR then lies between the ionised gas of the HII region and the neutral gas in which it is embedded, with a thin ionisation front between the two defining the region in which ionisation reduces from 100 per cent to zero, and in which dust dominates extinction.

Multiple indicators of the degree of ionisation within this front include bright atomic cooling lines (such as CI, CII, OI, and SII), fluorescent and thermal emission of rovibrational and pure rotational lines of H_2, polycyclic aromatic hydrocarbons (PAHs), dust mid- and far-IR continuum, and molecular rotational lines of CO, CN, HCN, and HCO^+, among others. Chapters 14 and 15 will look at those PDR molecular emissions in the high-flux and low-flux cases in more detail. For the moment, we can recognise that photon-induced chemistries are controlled by dust extinction as a function of depth in the cloud, with both distinct and mixed zones traced by different molecular species.

1.12 Masers

With clustered HMSF typically occurring at less than 1 pc separation, the gas kinematics can be thoroughly mixed up and complex to analyse. Being closely linked to a young, massive star's precise evolutionary stage, rotating accretion disks, bipolar outflows, expanding ionised hydrogen bubbles, and masers all contribute to our understanding of that stellar development process. Maser emission lines, being bright and highly beamed, are often used to trace the quite precise distance and proper motion measurements of these high-energy conditions. Masers are typically classified according to the conditions of their excitation. Those that highlight conditions where the radiant temperature is less than the kinetic temperature are likely to be collisionally pumped. Those that characterise conditions associated with proximity to UCHII regions or outflows, on the other hand, experience radiant temperature as the dominant cause of pumping. Engendered by the population inversion of already excited gas-phase molecules, common molecular masers include OH and SiO (radiatively pumped), H_2O (collisionally pumped), and CH_3OH (responsive to both pumping mechanisms and categorised as Class I and II, respectively). Factors such as velocity gradient as well as radiation field are intimately linked in maser formation, and we will consider those conditions of maser emission through many of the examples to come in the case studies.

https://doi.org/10.1017/9781009277433.002 Published online by Cambridge University Press

Molecular Astrophysics

1.13 Molecular Excitation

For a detailed account of molecular emission and absorption, the reader is directed to the Further Reading titles at the end of this chapter (Tielens, 2021, being particularly recommended). For the basics, suffice it to say that molecular astronomical observations in the gas phase depend upon the emission and absorptions arising from rovibrational transitions of interstellar and circumstellar molecules. Detailed theoretical knowledge of level populations, critical densities, molecular excitation temperatures, collisional de-excitation rates, and the optical depth dependence of each underpins all observational studies and is the prerequisite for determining the physical conditions associated with the star formation medium. The conditions in which emission enables astronomers to deduce likely chemical reaction networks are governed by temperature, density, ultraviolet photon field, and energetic ion (cosmic ray) flux. It is the relationship between these physical parameters and the molecular line emission to which they give rise that furthers our understanding of the interstellar medium generally and the star formation process in particular.

1.14 Level Populations

Interaction with photons or cosmic rays, and collisions with other molecules, atoms, or electrons, both induce molecular transitions. The simplest molecular cloud collisions are likely to be with ubiquitous H_2 or He. The resulting excitations involve jumps from lower- to higher-energy rotational quantised states, and the subsequent de-excitation and release of photons of a particular energy and wavelength present as line emission. Such emission occurs at a rate determined either by the Einstein A-coefficient, A_{ji}, for radiative de-excitation, or spontaneous radiative decay. The average time for spontaneous decay is $1/A_{ji}$. The equivalent coefficient for absorption between the same two levels is B_{ij}. Collisional de-excitation, with an energy transfer exclusively between collision partners, also occurs, in which case, again, no radiation is emitted.

1.15 Critical Densities and Excitation Temperatures

Where local thermodynamic equilibrium (LTE) prevails, the level populations are described by a Boltzmann distribution and the relative populations of the two levels are a simple function of temperature. Typically, molecular gas in the interstellar and circumstellar medium is not in LTE, and determining level

https://doi.org/10.1017/9781009277433.002 Published online by Cambridge University Press

populations requires we solve statistical equilibrium equations. In these calculations, above a critical particle density, collisions will dominate the de-excitation (and therefore observable emission) process. At densities below the critical density for each particular transition, each exciting collision is followed by a radiative de-excitation, so an upper-level population 'collapse' follows. If we define γ_{ji} as the rate coefficient for collisional de-excitation in the thermalised gas above critical density, then we can define that critical density for each specific transition as $n_{\rm cr} \sim A_{ji} / \gamma_{ji}$. Maximum emission efficiency typically occurs at gas densities close to critical, so even tracing non-uniform molecular cloud density is possible using different molecular species and different transitions. The excitation temperature, T_{ex}, of a given molecular transition is dependent upon the critical density; hence, where emission lines become visible, the critical density becomes an approximate particle density diagnostic, just as the excitation temperature serves as an approximation to the gas kinetic temperature.

Astrochemical Basics

1.16 Gas-Phase and Grain-Surface Reactions

Given the generally non-LTE conditions in interstellar and circumstellar molecular clouds, in which low-temperature and low-density gas is subject to high UV photon or energetic ion fluxes, the gas-phase chemistry is dominated by kinetic rather than thermodynamic factors. Reaction types and their reaction rates, and the factors that differentiate these, therefore largely determine the gas composition within a molecular cloud, with dust-surface reactions and gas–dust exchanges significantly supplementing the purely gas-phase chemical network under specific circumstances, such as close to newly forming stars. Most interstellar gas-phase reactions are bimolecular, with rates of formation and destruction determined by collision cross section as a function of velocity averaged over the velocity distribution of reaction partners. These bimolecular reactions include neutral–neutral, ion-neutral, charge transfer, and radiative association, while unimolecular reactions include photodissociation, and associative detachment. Appendix D gives some tabulated generic examples of rates for the variety of reaction types.

The factors determining gas–grain interactions and grain-surface processes involve accretion efficiency, sticking probability, binding energy, and surface mobility. Thereafter most reactions occur between radicals (species with

https://doi.org/10.1017/9781009277433.002 Published online by Cambridge University Press

unpaired electrons) depending upon activation energy barriers and tunneling probability factors. A variety of desorption mechanisms then arise in differing circumstances, driven by heat (thermal desorption), UV photons (photodesorption), local 'hot spots' arising from exothermic reactions (chemical desorption), shocks (sputtering), and heavy atom impacts (cosmic ray–driven desorption). Large, interstellar, carbon-based molecules composed of tens of atoms have their own specific chemistries. Polycyclic aromatic hydrocarbons (PAHs) are planar, fullerenes are spherical (e.g. the C_{60} 'soccer ball') or ellipsoid. When a PAH absorbs a UV photon, it acquires a high excitation temperature (~1,000 K) for a very short time (~1 s), emitting then in the IR region over an extended period (a day, month, or year, depending on how close to the emitting star) until it goes back down to ~10 K. While in an excited state, additional reactions can include ionisation or fragmentation into smaller hydrocarbons, plus reaction with other gas-phase species, particularly atomic H and electrons. For a standard text, Tielens (2021), listed under Further Reading at the end of this chapter, gives greater detail on these topics and is recommended.

1.17 Chemical Modelling

In attempting to match observation with theory, while there are variations in types of computational modelling of reaction networks in astrophysical environments – from steady-state single-point, through time-dependent single-point, to time-dependent depth-dependent, each exclusively gas-phase, grain-surface, or incorporating gas–grain exchange – all of them involve calculation of a set of rate equations as functions of particle abundance and time. These typically comprise systems of ordinary differential equations representing formation and loss of each species. Depending on the chosen application, inputs are likely to include initial elemental abundances, gas densities, gas temperatures, cosmic ray ionisation rates, radiation field strengths, dust extinctions, and perhaps freeze-out and desorption factors. All utilise a reaction database with its rate coefficients derived from both theory and experiment, with computations involving networks of thousands of atomic and molecular species. Appendix A directs the reader to examples of such databases. The output is usually a set of gas-phase or grain-surface fractional abundances for each species relative to hydrogen over a given time period, which for star formation studies is typically of most interest between 10^3 and 10^5 years.

https://doi.org/10.1017/9781009277433.002 Published online by Cambridge University Press

Observational Basics

1.18 Antenna Temperature and Optical Depth

Submillimetre and radio telescopes provide us with antenna temperatures, T_a, which we relate to fundamental molecular constants and astronomical parameters such as column densities, number densities, and gas temperatures. Even in the simple case of LTE , where level populations are dominated by collisions in gas at uniform temperature, the derivations for linear and non-linear molecules are different and best studied in detail in a standard text (that of Williams & Viti, 2013, referenced in Further Reading, being an excellent example). The relationship between T_a at frequency v and optical depth τ can be given by the following equation:

$$\tau = h/\triangle v\left\{N_u B_{ul}(e^{hv/kT}-1)\right\},$$

where N_u is the column density of the upper state and Δv is the full width at half-maximum line width in units of velocity. The optical depth is computed by considering the probability that the emitted photon may escape from the locality, allowing for an absorption at a rate $B_{ul}\rho$, where B_{ul} is the Einstein coefficient for radiatively induced de-excitation and ρ is the energy density. Using standard equations (for which again derivations can be found in standard texts), given that the ratio of Einstein coefficients is expressible as

$$A_{ul} / B_{ul} = 8\pi hv^3 / c^3$$

and the relationship between antenna temperature and optical depth is expressible as

$$T_a = hc^3 N_u A_{ul}/8\pi kv^2 \triangle v(\triangle\Omega_s/\triangle\Omega_a)(1-e^{-\tau}/\tau)\tau,$$

we can also find

$$N_u = 8\pi kv^2\Omega / hc^3 A_{ul}(\triangle\Omega_\alpha/\triangle\Omega_\sigma)(\tau/1-e^{-\tau}),$$

in which the omega terms are source and antenna solid angles.

In summary, optically thin transitions will give telescope antenna temperatures proportional to the column density in the upper level of the emission transition observed. If we assume all the transitions are thermalised and that we know the kinetic temperature, the column density derived from the single transition can be equated with the total column density for the species. If the emission is optically thick, then the opacity results in an underestimate of the upper-level column density as well as the molecular rotational temperature. In fact, degrees of optical depth can be deduced from a rotation diagram analysis

https://doi.org/10.1017/9781009277433.002 Published online by Cambridge University Press

for both the LTE case and, with corrections, the non-LTE case. Before briefly looking at this, we should be sure of the following observational basics.

1.19 Velocity Distribution

Velocity maps are widely used to separate out different gas components from one another. Gas clouds are invariably moving, and in particularly complex ways close to newly forming stars. We look for measurable shifts in the observed emission or absorption lines relative to our local standard of rest. The mean speed of Galactic rotation in our stellar neighbourhood is ~250 km s^{-1}. There is also a peculiar Solar motion with respect to that ~16.5 km s^{-1}. Earth is locked into that rest frame, and relative to it, along a line of sight we may observe red- or blue-shifted lines. A numerically positive velocity difference indicates gas receding from us, and a negative shift indicates gas approaching. However, unless the gas movement is directly towards or away from us precisely aligned along the line of sight, these are not 'actual' relative velocities. Most movement will be somewhere between line of sight and plane of sky projection. However, most important is the fact that emissions from different species that show the same velocity shift are likely to be in the same spatial location.

1.20 Column Density, Beam Dilution, and Relative Abundance

Three simple constraints fundamental to observational astronomy are column density, beam dilution, and relative abundance. Imagine we look down a 100 cm-length tube with a 1 cm-diameter circular cross section and see 100 particles. Assuming an even distribution of particles inside the tube, from the formula for the volume of a cylinder ($h\pi r^2$) we deduce an average of 1 particle in every 0.78 cm^3 of space, which is the 'volume density'. Take that volume density and multiply it by the tube length and we have the 'column density', which in this case is 0.78 $cm^{-3} \times 100$ cm = 78 cm^{-2}. We have assumed an even distribution of particles along the length of the tube, but, of course, the column density would be the same even if all the particles are crowded together at the far end. That is the problem facing the astronomer observing along a line of sight – working out where exactly along that telescope beam the particles are actually distributed. Comparative velocity distribution among molecular species becomes essential information in that analysis.

https://doi.org/10.1017/9781009277433.002 Published online by Cambridge University Press

Having decided that a range of evidence points to the location of the particles exclusively towards the end of our beam, if the telescope beam is larger than the observed object itself, then the extent of 'beam dilution' will influence our estimation of particle volume density at that location. For example, observing a hot core having a dimension less than 1 or 2 arcseconds against the sky with a single dish telescope limited to perhaps 20–30 arcseconds resolution restricts column density estimates to very approximate lower limits. Given the uncertainties, we might prefer to simply express the column density of one particle species as a fraction of another that we know to exist in the same place. Since molecular hydrogen is far and away the most abundant species in dense molecular gas, the fractional abundance of all other species can be expressed in relation to it. For example, the first major detection of ethanol in the Galaxy beyond Earth's atmosphere was made towards the G34.26+0.15 hot core (Chapter 12). In this case, the column densities of ethanol (C_2H_5OH) and H_2 were deduced to be 10^{15} cm^{-2} and 10^{23} cm^{-2} respectively, hence a fractional abundance for ethanol of $10^{15}/10^{23} = 10^{-8}$. Among the following case studies, fractional abundances of other paired species, including directly related species such as chemical product to precursor, will enter the discussion.

1.21 Rotation Diagrams

One commonly used technique among observers is the rotation diagram analysis in which, assuming LTE in the first instance, at temperature T_k the column density of each populated upper level u is related to the total column density via

$$N_u = N / Z\left(g_u e^{-Eu/kTk}\right),$$

where N is the total column density of the species, Z is the partition function, g_u is the statistical weight of the level u, and E_u is the energy above ground state. Thus, all we need to deduce total column density is an observed temperature. If we have multiple transitions for the same species, then we can construct a rotation diagram relating column density per statistical weight of multiple molecular energy levels to their energy above ground state. The rotation diagram plots the natural logarithm of N_u / g_u versus E_u / k. For the LTE condition, the plot would be a straight line with a negative slope of $1 / T_k$. This derived rotation temperature is expected to equal the kinetic temperature, as we have said, for the thermalised gas case. However, most astrophysical conditions are not ideal LTE cases, and the opacities for individual transitions in given circumstances are far from known. Negotiating these and other difficulties in order to extract

https://doi.org/10.1017/9781009277433.002 Published online by Cambridge University Press

reliable information is a complex business, but the many rotational lines of the many molecular species in a cloud, each with their own critical density and excitation energy, in principle offer astronomers powerful diagnostic tools for interpreting physical conditions.

1.22 Radiative Transfer Modelling

In the analysis and interpretation of observations where LTE is too gross an approximation, we consider all the individual excitation and de-excitation processes, collisional and radiative, through statistical equilibrium calculations. Provided collisional data is available, line radiative transfer models permit the calculation of level populations that underpin output spectra. The codes typically compute flux or intensity of individual line emission, and output line profiles. The assumptions are that temperature, density, and abundance are constant, since these determine the collisional coefficients, the level populations, and hence the emission. In non-LTE conditions, the excitation temperatures in particular are critical in determining level populations, so alternative approximations, such as LVG (large velocity gradient) radiative transfer modelling, are often used. Just as the rate coefficients are the major uncertainty in chemical modelling, the collisional coefficients are the principal uncertainties in LVG modelling. Other methods have been developed to solve, ever more accurately, the radiative transfer problem, and the interested reader is invited to start with Williams and Viti (2013) and the references therein.

Further Reading

Molecular Astrophysics, A. G. G. M. Tielens, Cambridge University Press (CUP) 2021: The most comprehensive account of molecular astrophysics available, connecting molecular physics, astronomy, and physical chemistry. The best current standard textbook.

Observational Molecular Astronomy, D. A. Williams & S. Viti, CUP 2013: An excellent introduction to observational techniques at millimetre and submillimetre wavelengths and the extraction of useful astronomical information from raw telescope data.

The Physics & Chemistry of the Interstellar Medium, A. G. G. M. Tielens, CUP 2006: An overview of the theoretical and observational understanding of the ISM, offering greater detail than *Case Studies* on the microscopic physical and chemical processes that influence macroscopic interstellar structures.

An Introduction to Star Formation, D. Ward-Thompson & A. P. Whitworth, CUP 2011: An excellent overview of the wider aspects of star formation, comprehensive and concise.